SAFE OPERATIONAL BANDWIDTH OF GAS STORAGE RESERVOIRS
WP7 REPORT
PHASE 1 & PHASE 2 FINAL REPORT

Pietro Teatini
Claudia Zoccarato
Massimiliano Ferronato
Andrea Franceschini
Giovanni Isotton
Matteo Frigo
Carlo Janna

Padova, January 2019

DIPARTIMENTO DI INGEGNERIA CIVILE, EDILE E AMBIENTALE - I C E A
DEPARTMENT OF CIVIL, ENVIRONMENTAL AND ARCHITECTURAL ENGINEERING

Contents

1. Introduction

The project “Safe operational bandwidth of gas storage reservoirs” is aimed at investigating the geomechanical hazards and risks associated with gas storage in Underground Gas Storage (UGS) reservoirs. In particular, the aim of the research activities is to investigate how possible drivers of fault reactivation can combine in UGS to increase the hazard of (significant) seismic events and/or even induced "un-expected" (micro-) seismicity.

The project has been developed within two phases, with the activities distributed in seven Work Packages (WPs) as briefly summarized here:

Phase 1:

WP1– Bibliographic review. A bibliographic review of the most recent scientific publications has been carried out to develop an inventory of possible mechanisms of fault reactivation induced by fluid injection/production into/from deep reservoirs. Seismic occurrences have been subdivided according to the reservoir development stage, i.e. primary production (PP), cushion gas injection (CG), and UGS, the event focal mechanism and magnitude, and the hypocentre location with respect to the developed formation (below, at the same depth, above);

WP2 – Conceptual model and definition of the potential driving mechanisms. The conceptual model and mechanisms possibly causing fault reactivation have been defined based on the WP1 outcome. The analysis has addressed the role of (i) the geological settings, such as the geometric configuration and the hydro-geomechanical properties of faults and reservoir, (ii) the poro-elastic stress changes with respect to the natural stress regime, and (iii) the space and time pore pressure gradients in the UGS formation and within the faults bounding/compartmentalizing the reservoir;

WP3 – Modelling scenarios. Based on the WP2 outcome, the modelling set-up has been defined and the scenarios and mechanisms of fault reactivation proposed in WP2 investigated using the M3E_GEPS3D geomechanical simulator. The simulations have been carried out on a simplified geologic setting in terms of both reservoir and fault geometry (Figure 1) and a pressure history representative of the typical UGS reservoirs in The Netherlands: a ten-year production phase when the reservoir experiences a maximum pressure change ΔP = - 200 bar is followed by a 2-year CG phase during which the reservoir recovers the initial pressure and a UGS cycle spanning one year with a 6-month production phase (ΔP = - 100 bar) and 6-month of gas storage causing the recovery of the initial pressure. A 1-year loading step is used during PP and CG, while during UGS the loading step is equal to 0.1 year. The Norg and Bergermeer UGS fields have represented the “reference” for this modelling application. Faults have been simulated using an interface element approach with the hypothesis of “sealing conditions”, i.e., the pore pressure within the fault (between the two contact surfaces) does not change with respect to the initial value. This is the most critical condition in relation to fault re-activation;

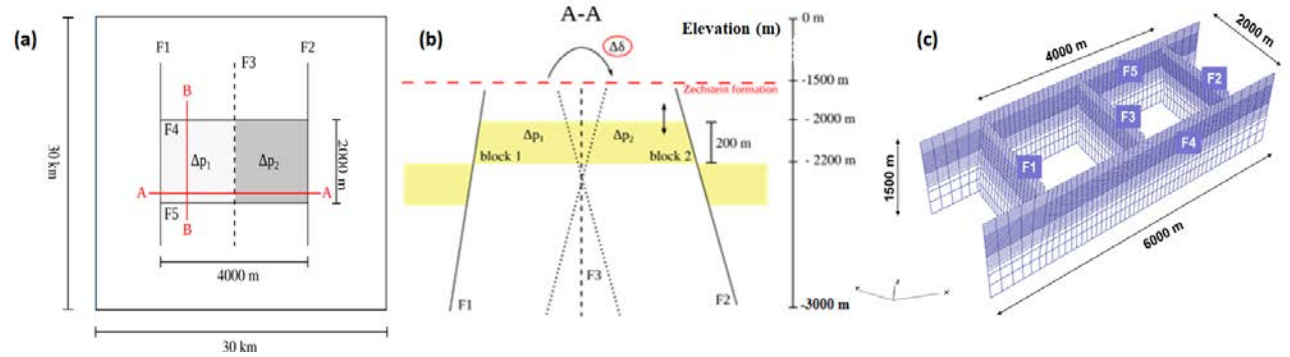

Figure 1 Geological setting used in the study: (a) plan view of the model with the main planar dimensions; (b) vertical section of the model along the trace A-A shown in (a) with the main information about reservoir and fault depth; and (c) perspective view of the IE discretization of the fault discontinuities: F1, F2 and F3 are parallel to the y-axis whereas F4 and F5 to the x-axis. F3 is the central fault subdividing the reservoir into two compartments.

WP4 – Analysis of modelling results. The main achievements obtained by the various simulations carried out in WP3 have been processed with the aim of (i) ranking the simulated scenarios in relation to their possibility of inducing unexpected seismic events during cushion gas injection and UGS cycles, (ii) weighting the critical factors (drivers / settings) influencing fault activation during UGS cycles, thus understanding which are the mechanisms most prone to cause unexpected seismic events during UGS activities, and (iii) anticipating a few preliminary notes on possible guidelines for safe operational bandwidths.

Phase 2: this second part of the project represents a Phase 1 follow-up. The opportunity of this integration emerged to relax the Phase 1 assumption that the pressure change does not propagate from the reservoir blocks into the surrounding/intercepting faults. Moreover, other two updates have been implemented: (i) the Zechstein formation sealing the reservoir has been characterized by a more accurate property distribution; and (ii) the computation of the fault criticality index χ has been conducted at the element level (rather than at the node-level) to mitigate the effect of the unphysical abrupt change of the pore pressure that sharply decreases within the reservoir and keeps the initial value within the caprock. By this way, the need of a 3D FE-IE mesh refinement along the vertical direction with a smoother distribution of the pressure change at the reservoir top and bottom has been overcome. Phase 2 is made of the following WPs:

WP5 – Testing the proposed updates. The effect of the various modifications has been tested and the updated "reference" scenario has been defined;

WP6 – Modelling scenarios. The scenarios investigated in WP3 have been re-evaluated taking into account the pressure change within the faults and the updated features of the salt caprock. A few more combined mechanisms have been investigated;

WP7 – Final report. Based on the previous outcomes, in particular the numerical results provided in WP3, WP5 and WP6, the report aims at providing a few general rules to define a "safe operational bandwidth of gas storage reservoirs".

As recalled just above, the outcomes of the various scenarios investigated in WP3, WP5, and WP6 have been processed in this WP7 to provide the final result of the project. The activities carried out in this last part of the study can be split as follows:

- comparison of the simulated scenarios;
- comparison of the results obtained in this study with recent published outcomes;
- rank the simulated scenarios in relation to their possibility of inducing unexpected seismic events during cushion gas injection and UGS cycles;
- weight the critical factors (drivers / settings) influencing fault activation during UGS cycles; i.e., understanding which are the mechanisms most prone to cause unexpected seismic events during UGS activities;
- development of a few general guidelines for safe operational bandwidths based on the study outcomes.

2. Comparing scenarios

Several scenarios have been investigated in WP6. Here, their outcomes are cross-compared to point out which are the parameters and/or geometric features making the subsurface system more prone to fault reactivation.

Specifically, we have elected to use t_{80} (i.e., the faults thickness with a node-base criticality index > 0.8) as the parameter more representative to carry out this analysis. Moreover, we have focused the investigation on the central fault F3, which is the most stressed in realistic conditions, and fault F2 that is representative of the discontinuities bounding the reservoir. The stress conditions on faults F4 and F5 are generally less critical because of the initial stress regime (excluding scenario 4a), the fault verticality, and the constant depth (lack of offset) of the various portions of the Upper Rotliegend along the direction orthogonal to F4 and F5.

The comparison is provided in Figure 2 to Figure 5. Inspection of these figures, together with element-based χ_{max} and δ_{max} behaviours provided in WP6 Report, allows pointing out the following:

- the initial stress regime can play a major role: decreasing significantly the horizontal principal components (as tested in scenario 4b that is characterized by $M_1 = 0.40$ and $M_2 = 0.47$, i.e. almost half of the most likely values) favours an early fault reactivation, with a large area critically stressed and significant sliding between the two fault walls. The fault areas in a critical stress state increase during the last part of CG as well as the end of UGS production and injection phases;
- apart from this (unlikely) setting, the following are the four main factors yielding (a portion of) the faults close to a critical stress state also during CG and UGS (generally at the end of the injection / production phases when the pressure change – both decreasing and increasing –reaches the largest value): a reduced friction angle (scenarios 5b, 5c, 11); an increased offset between producing compartments (scenario 3d); a large difference between the reservoir stiffness and that characterizing the caprock, sideburden, and underburden (scenario 6a vs 6b, and scenario 11 vs 14); and an uneven pressure change within adjacent compartments (scenarios 7a, 7b);

- the scenarios causing fault reactivation during primary production are more prone to fault failure during cushion gas injection and UGS. Indeed, reversing the sign of the pressure change when only elastic deformations developed (i.e., no fault has been activated) causes the system to be unloaded, returning to the original regime. Conversely, fault activation during primary production (generally at the end of this development phase in the scenarios addressed in this study) leads to a stress redistribution and a new (deformed) "equilibrated" configuration that is newly loaded, in the opposite direction, when the pressure variation changes the sign.

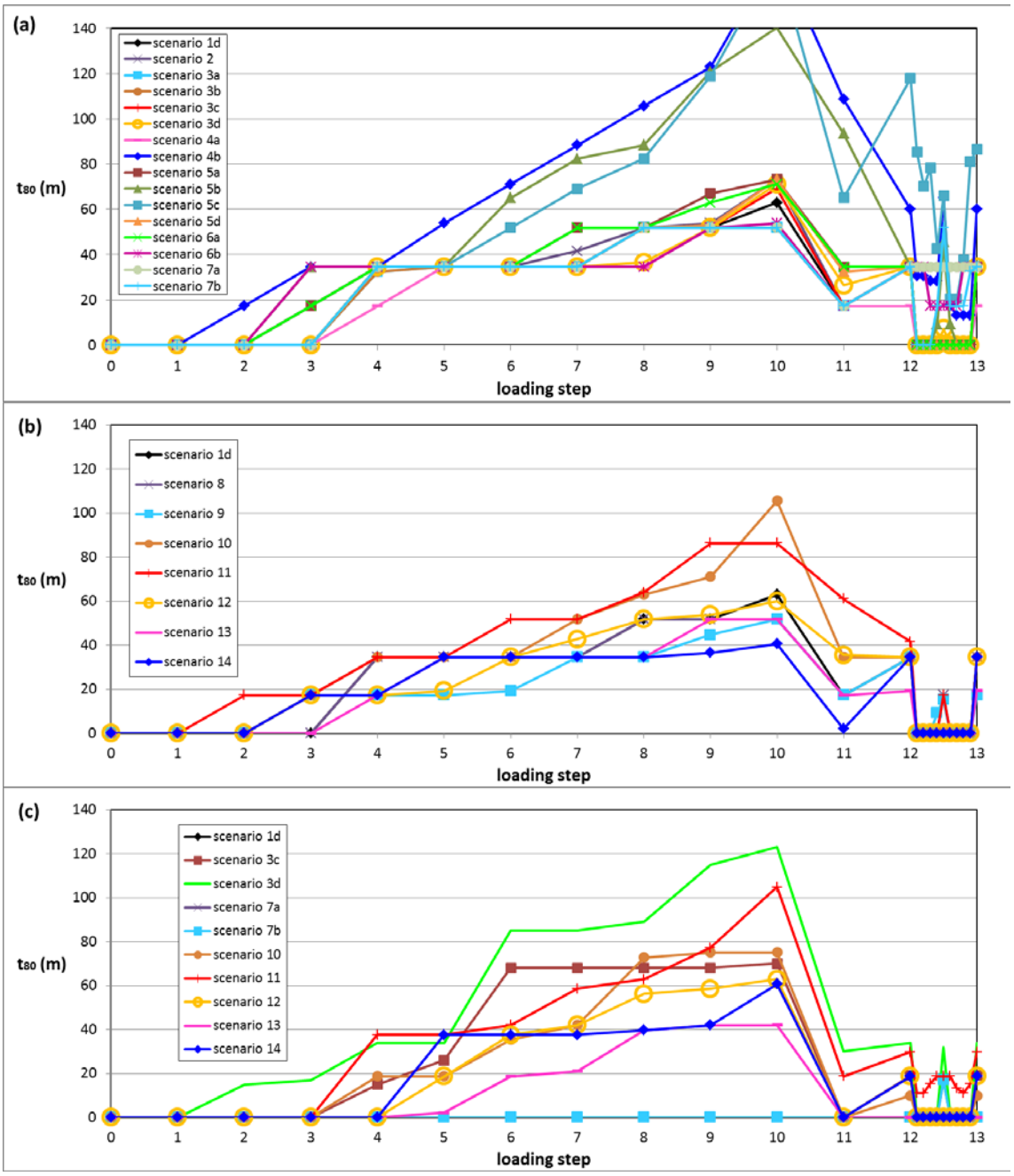

Figure 2 Comparison between the t_{80} time behaviors obtained with: (a) fault F2, scenarios investigated in the sensitivity analysis; (b) fault F2, combined scenarios; and (c) fault F3, scenarios with asymmetry in the geological setting and/or stress driving forces. The profiles refer to the entire simulated period: primary production between loading steps #0 to #10, cushion gas injection from loading steps #10 to #12, and UGS between loading steps #12 to #13.

It must be recalled that the IEs in correspondence of the reservoir depth interval are 100-m wide and 20-m thick. This is the reason why the t_{80} curves in Figure 2 to Figure 5 generally change with a ~20-m step. However, a certain deviation can occur in few scenarios due to the three-dimensionality of the system (with a certain difference between the fault behaviour in correspondence of the block centre respect to the corners) and the fixed normalization factor (the entire fault/block length, i.e. 2000 m for F1, F2 and F3) used to compute the thickness from the area of the IEs with χ above the selected threshold.

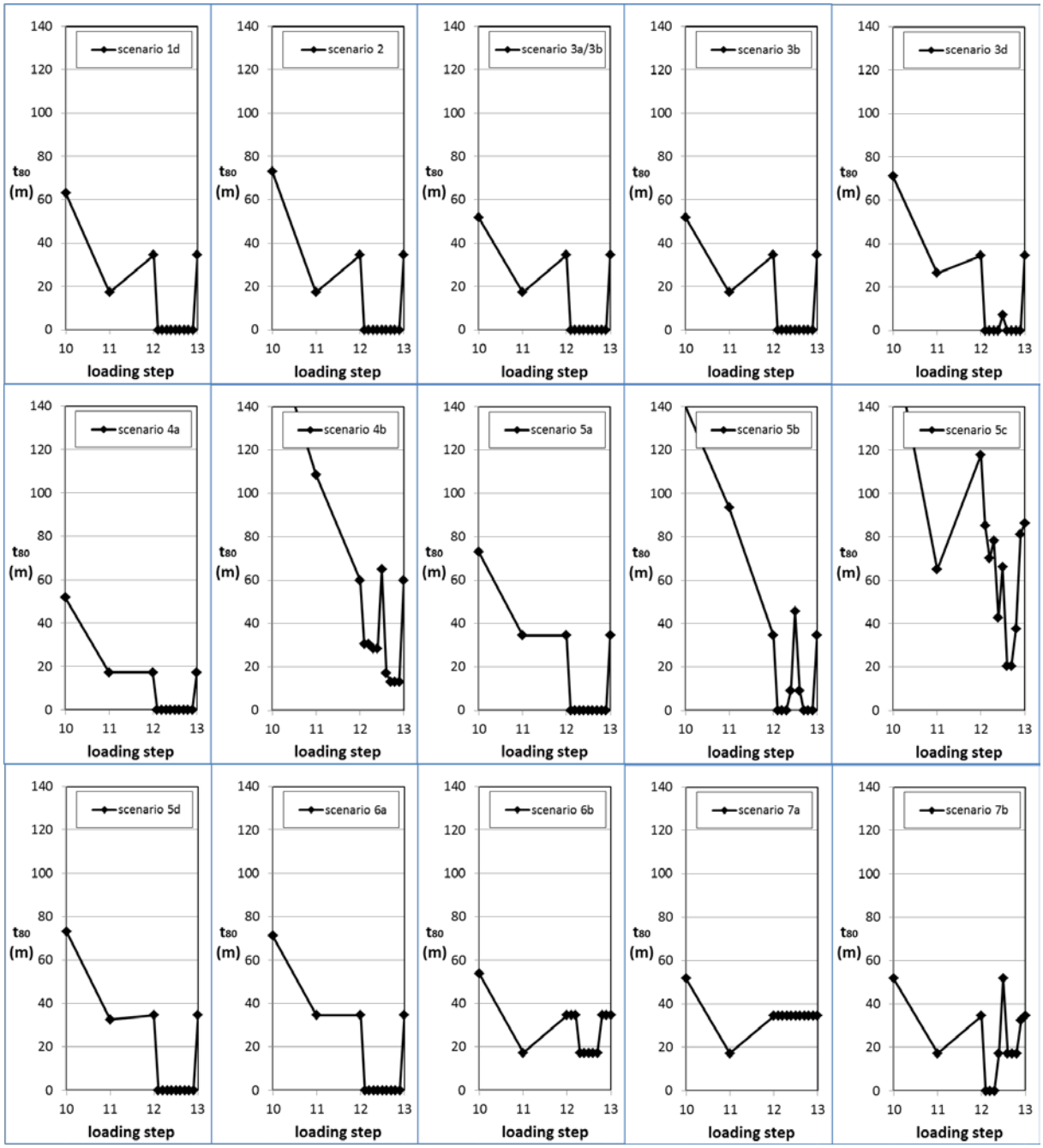

Figure 3 Fault F2: comparison between the t_{80} time behaviors obtained in the scenarios investigated with the sensitivity analysis. The profiles refer to cushion gas injection (loading steps from #10 to #12) and UGS (loading steps from #12 to #13) phases.

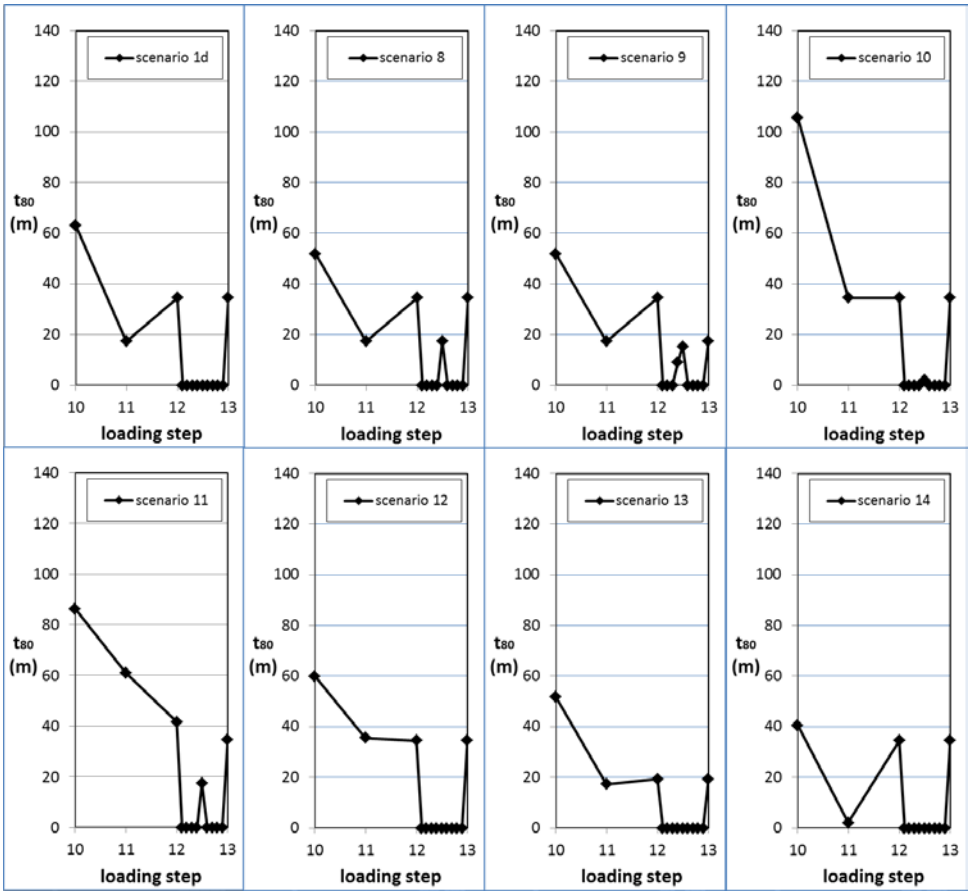

Figure 4 Fault F2: comparison between the t_{80} time behaviors obtained with the combination scenarios carried out in WP6. The profiles refer to cushion gas injection (loading steps from #10 to #12) and UGS (loading steps from #12 to #13) phases.

Other observations worth to be highlighted and specifically related to UGS, are:

- it is interesting to compare scenarios 7a and 7b, fault F2 (Figure 3). The two scenarios are characterized by the same history until the end of CG injection and then the difference is quite significant. When $\Delta P_2 = 0$ (scenario 7a), fault F2 keeps the degree of criticality matured at the CG end over the entire UGS phase. In scenario 7b ($\Delta P_2 = -200$ bar), UGS production initially unloads F2 respect to the CG end and then loads it again with its activation at loading step #12.5 (Figures 23 and 24b, WP6 Report) when the maximum UGS depletion is reached. The consequent new configuration is then initially unloaded during the first part of UGS injection, but then loaded again when the pressure increase reaches large value, with a new reactivation at loading steps #12.9 and #13;
- scenario 11 (combination 2) is particularly critical during UGS for faults F2 (Figure 4) and, even more, F3 (Figure 5). The superposition of a compartment offset, with a relatively small friction angle, and a viscous caprock leads the two faults to increase their critical condition also at the end of the UGS production phase (and not only at the end of the injection phase).

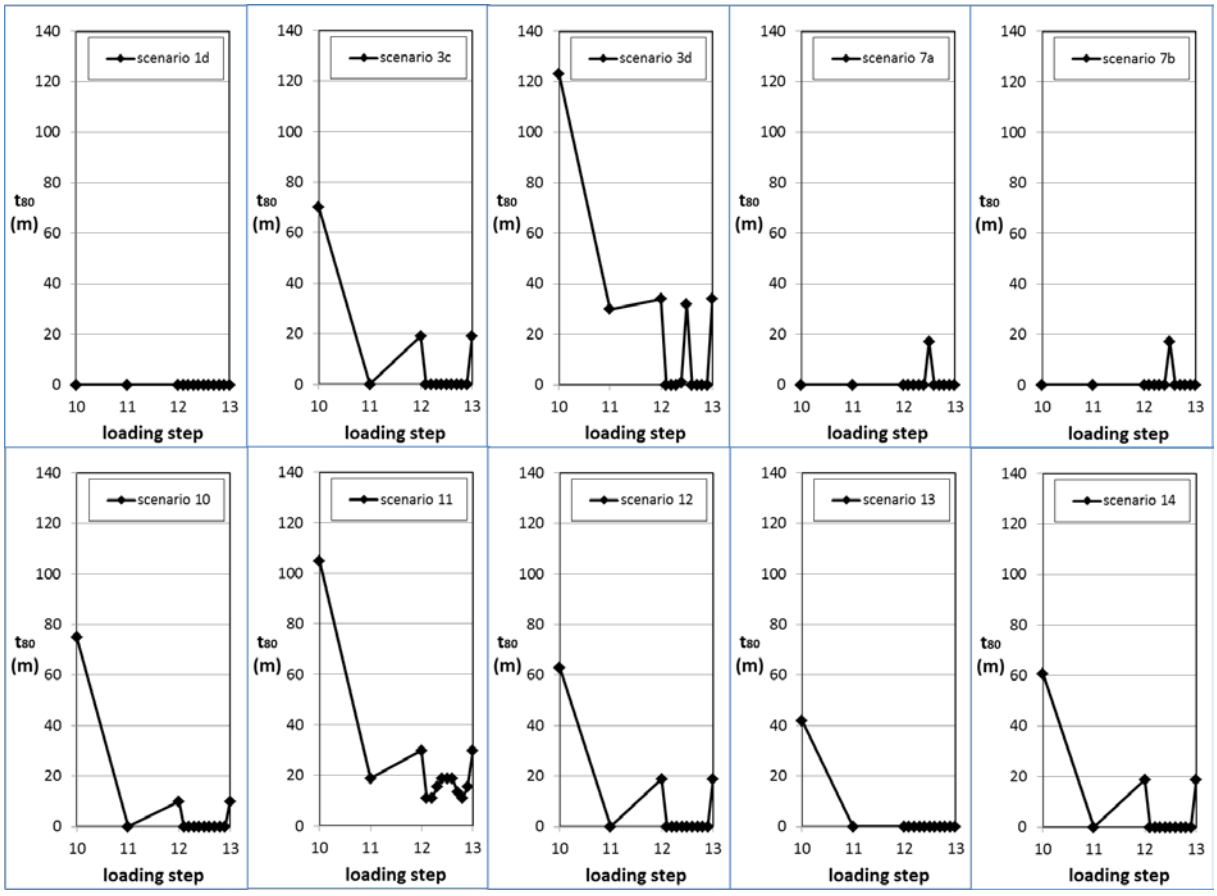

Figure 5 Fault F3: comparison between the t_{80} time behaviors obtained with the scenarios where the fault is loaded by shear stress because of asymmetry in the geological setting and/or driving forces. The profiles refer to cushion gas injection (loading steps from #10 to #12) and UGS (loading steps from #12 to #13) phases.

3. Comparison with recent published outcomes

A few papers addressing the topics of this project have been published during the last few years. A couple of them:

- Wassing, B.B.T., L. Buijze, J.H. Ter Heege, B. Orlic, S. Osinga, The impact of viscoelastic caprock on fault reactivation and fault rupture in producing gas fields. 51st U.S. Rock Mechanics/Geomechanics Symposium, Paper # ARMA-2017-0355, American Rock Mechanics Association, 2017;
- Haug, C., J.-A. Nüchter, A. Henk, Assessment of geological factors potentially affecting production-induced seismicity in North German gas fields. Geomechanics for Energy and the Environment, 16, 15-31, 2018;

are of particular interest because they are focused on Rotliegend reservoirs in the Netherlands and in northern Germany. Although they i) focus on induced seismicity during primary production and not specifically on UGS reservoirs, ii) use a 2D model set-up, and iii) a different modelling approach in relation to fault activation, these studies carry out a parametric analysis on the same geometric/geomechanical features investigated in this project. Therefore, it is interesting to see if

our results conform to those presented in these publications. The comparison is summarized in Table 1 and Table 2.

Table 1 Main findings from Wassing et al. (2017) and their agreement/disagreement with the results of this project

"due to the decrease in pore pressure, a uniform increase in shear stress, normal effective stress and SCU is observed on the fault segment which intersects the reservoir rocks. As initial SCU (i.e., χ) is highest at the top of the reservoir block, fault slip starts at the top of the reservoir rocks"	**agreement** our study reproduces the same mechanism of fault failure
"a second, albeit smaller, peak in shear stress is observed at the bottom of the footwall reservoir block ... On the other hand, a very localized decrease in shear stresses and SCU is observed at a depth of 3100 m, at the bottom of the hanging wall reservoir block"	**agreement** at least from a qualitative point of view. It must be considered that Wassing at al. assigned uniform density and elastic properties to all rock. We have demonstrated that the contrast in the elastic properties distribution plays a major role in stress concentration and, therefore, fault failure
"the viscoelastic creep behavior of the halite caprock further promotes fault reactivation and causes fault rupture at an early stage of depletion"	**partial agreement** viscous creep favours fault reactivation also in our results although to a lesser degree. The difference can be due to initialization and timing that largely differ in the two modelling approaches. In our study, the viscoelastic caprock promotes a more critical fault condition at later UGS cycles
"Faults without offset are reactivated at later stages of depletion"	**agreement** our results confirm this statement. Fault offset favours an earlier fault reactivation
"In none of the cases modelled, fault rupture extended upwards into the Zechstein caprock."	**agreement** our study provides the same results, with the fault activation that is bounded within the reservoir depth range also in the case of block offset

Summarizing, despite the different parametrization, Wessing et al. (2017) and our outcomes agree in reproducing the mechanisms of fault failure and in the role plays the viscous caprock. A main difference, which would require a specific and more in-depth investigation to be fully understood (e.g., which is the role exerted by the reservoir overpressure, a parameter not accounted for in our investigation), is related to the initial condition of the fault stress regime when a block offset characterize the reservoir geometry. According to Wessing et al. (2017), "*for the fault with 100 m offset, initial conditions on the fault at a depth of 2900 m are already critical*"; this initial critical state in not observed in our modelling set-up. Notice that this study is not specifically focused on the effect exerted by a viscous caprock.

Table 2 Main findings from Haug et al. (2018) and their agreement/disagreement with the results of this project

"we find that large Biot–Willis coefficients are more favourable for fault reactivation"	**agreement** our results confirm this statement: the use of α=1 yields to a more critical condition in terms of possible fault failure
"an increasing horizontal (pre-production tectonic) compressive stress counteracts normal faulting so that the impact of production on fault criticality is reduced"	**agreement** our results confirm this statement: the initial stress regime plays a major role and fault criticality largely increases as the horizontal components of the natural stress regime decrease relative to the vertical stress
“the stiffness contrast between reservoir and surrounding rocks governs the distribution of the production-induced loading and the degree of rotation of the principal stresses being favourable or unfavourable for fault reactivation with pore fluid pressure depletion”	**agreement** Similar results have been obtained in our analyses. Stiffness contrast plays a major role in stress redistribution, generally favouring fault reactivation when the contrast increases
"On the intra-field fault, significant loading occurs for a setting where reservoir compartments are partly juxtaposed"	**agreement** offset of reservoir blocks increases significantly the intra-field fault criticality also in our results
"maximum SSR values are obtained for the case that fault throw is half of the reservoir thickness "	**partial disagreement** in our results the most critical condition is obtained with a fault offset equal to the entire reservoir thickness. This difference can be explained by the unlike set-up of the two models. In particular: i) the different horizontal to vertical ratio of the natural stress components and ii) the reservoir depth (4800 vs 2000 m). According to Geertsma’s model, a larger upward displacement of the reservoir bottom occurs when the reservoir is shallower
"maximum SSR values are obtained for the case that production is exclusively from the footwall"	**partial agreement** this is not uniquely defined in our results that are wider on this aspect
"depletion of thick reservoir horizons results in a stronger fault-loading compared to the depletion of thinner reservoir horizons as the thick reservoir undergoes a relatively larger strain for the same pore fluid pressure decrease"	**agreement** although not directly simulated (the reservoir thickness is not a parameter addressed by our sensitivity analysis), we have consistent results when the larger strain is due to a larger pressure decrease
"the stress state below the transition of a salt diapir’s flanks to source layer is favourable for fault reactivation due to locally increased vertical stress"	**partial agreement** viscous caprock increases critical stress state, however the geometry of the viscous layer is very different in the two models

4. Ranking scenarios

A first task concerns the possibility of ranking the mechanisms, geological settings, geomechanical and production parameters in relation to their potentiality of inducing "unexpected" seismic events. The sensitivity scenarios and the various mechanisms have been ranked following these nested criteria:

1. (a) element-based χ_{max} during UGS; or (b) $\chi^* = \sum_{element}(t_e \cdot \chi|_{\chi>0.8})$ normalized over $\max(\chi^*)|_{scenarios}$ where t_e is the element thickness (more generally the element area if a non-regular discretization is used);
2. maximum value of average sliding (δ_{avg}), evaluated on active elements only;
3. loading step of activation.

The analysis has been carried for the central fault F3, which is the most stressed in realistic conditions, and fault F2 that is representative of the discontinuities bounding the reservoir. Notice that fault F3 is inactive in some of the investigated scenarios because of symmetry in the geological setting and driving forces. The ranking has involved the two reference cases (scenario 1a, i.e. the Phase 1 reference case, and scenario 1d, i.e. the Phase 2 reference case), the various sensitivity, mechanisms and combined scenarios investigated in WP6 and the most significant WP3 scenarios not addressed in WP6: the scenario with a cohesion equal to 100 bar, COMB_1_PF, and COMB_2_PF. In order to guarantee consistency, the WP3 outcomes have been reprocessed to evaluate χ on an element base. The results of the two ranking procedures are reported in Table 3 and Table 4 for fault F2, and in Table 5 and Table 6 for fault F3. A classification has been also carried for the combination scenarios, see Table 7.

Table 3 Fault F2: ranking of the simulated scenarios, from the most to the least prone to induce fault reactivation during cushion gas injection and UGS phases, using criterion 1(a)

Scenario #	Parameter / Mechanism	χ_{max} UGS	Maximum δ_{avg}	Activation L.S.	χ_{max}
5c	φ_d = 10° ; d_c = 2 mm	1.00	0.026	7	1
7b	ΔP1 = -100 bar; ΔP2 = -200 bar	0.97	0.010	9	1
4b	M1-M2 lower	0.96	0.018	6	1
3d	offset = 200 m	0.84	0.008	9	1
5b	φ_s = 20°	0.81	0.010	7	1
3c	offset = 100 m	0.80	0.007	9	1
6a	E = 8 GPa	0.79	0.010	8	1
5a	c = 0 bar	0.78	0.008	8	1
1d	new reference	0.78	0.007	8	1
7a	ΔP1 = -100 bar; ΔP2 = 0 bar	0.78	0.007	9	1
8	UGS ΔP1 = ΔP2 = -150 bar	0.78	0.007	9	1
6b	E = 20 Gpa	0.78	0.005	-	0.79
3a/b	F3 dip = 65°	0.77	0.007	8	1
2	Biot = 1.0	0.76	0.008	8	1
4a	θ = 90°	0.74	0.007	10	1
9	viscous salt caprock	0.70	0.009	10	1
5d	φ_d = 20° ; d_c = 20 mm	0.70	0.009	8	1
1a	old reference	0.64	0.007	-	0.89
5b WP3	c =100 bar	0.34	0.003	-	0.6

Table 4 Fault F2: ranking of the simulated scenarios, from the most to the least prone to induce fault reactivation during cushion gas injection and UGS phases, using criterion 1(b)

Scenario #	Parameter / Mechanism	χ^*	Maximum δ_{avg}	Activation L.S.	χ_{max}
4b	M1-M2 lower	1.00	0.018	6	1
5c	φ_d = 10° ; d_c = 2 mm	0.62	0.026	7	1
7b	ΔP1 = -100 bar; ΔP2 = -200 bar	0.52	0.010	9	1
5b	φ_s = 20°	0.51	0.010	7	1
8	UGS ΔP1 = ΔP2 = -150 bar	0.39	0.007	9	1
5a	c = 0 bar	0.29	0.008	8	1
6a	E = 8 GPa	0.27	0.010	8	1
3d	offset = 200 m	0.26	0.008	9	1
3c	offset = 100 m	0.26	0.007	9	1
7a	ΔP1 = -100 bar; ΔP2 = 0 bar	0.26	0.007	9	1
3a/b	F3 dip = 65°	0.26	0.007	8	1
2	Biot = 1.0	0.25	0.008	8	1
5d	φ_d = 20° ; d_c = 20 mm	0.23	0.009	8	1
4a	θ = 90°	0.22	0.007	10	1
6b	E = 20 GPa	0.17	0.005	-	0.79
9	viscous salt caprock	0.17	0.009	10	1
1a	old reference	0.16	0.007	-	0.89
1d	new reference	0.15	0.007	8	1
5b WP3	c = 100 bar	0.00	0.003	-	0.6

Table 5 Fault F3: ranking of the simulated scenarios, from the most to the least prone to induce fault reactivation during cushion gas injection and UGS phases, using criterion 1(a)

Scenario #	Parameter / Mechanism	χ_{max} UGS	Maximum δ_{avg}	Activation L.S.	χ_{max}
3d	offset = 200 m	0.84	0.033	7	1
3c	offset = 100 m	0.81	0.007	-	0.85
7a	ΔP1 = -100 bar; ΔP2 = 0 bar	0.53	0.000	-	0.53
7b	ΔP1 = -100 bar; ΔP2 = -200 bar	0.53	0.000	-	0.53
3a/b	F3 dip = 65°	0.32	0.000	-	0.46
2	Biot	0.00	0.000	-	0
4a	theta = 90°	0.00	0.000	-	0
4b	M1-M2 lower	0.00	0.000	-	0
5a	c = 0 bar	0.00	0.000	-	0
5b	φ_s = 20°	0.00	0.000	-	0
5c	φ_d = 10° ; d_c = 2 mm	0.00	0.000	-	0
5d	φ_d = 20° ; d_c = 20 mm	0.00	0.000	-	0
6a	E = 8 GPa	0.00	0.000	-	0
6b	E = 20 GPa	0.00	0.000	-	0
8	UGS ΔP1 = ΔP2 = -150 bar (mech 04)	0.00	0.000	-	0
9	salt caprock	0.00	0.000	-	0
1a	old reference	0.00	0.000	-	0
1d	new reference	0.00	0.000	-	0
5b WP3	c =100 bar	0.00	0.000	-	0

Table 6 Fault F3: ranking of the simulated scenarios, from the most to the least prone to induce fault reactivation during cushion gas injection and UGS phases, using criterion 1(b)

Scenario #	Parameter / Mechanism	χ^*	Maximum δ_{avg}	Activation L.S.	χ_{max}
3d	offset = 200 m	1.00	0.033	7	1
3c	offset = 100 m	0.71	0.007	-	0.85
3a/b	F3 dip = 65°	0.50	0.000	-	0.46
7b	ΔP1 = -100 bar; ΔP2 = -200 bar	0.31	0.000	-	0.53
7a	ΔP1 = -100 bar; ΔP2 = 0 bar	0.29	0.000	-	0.53
2	Biot	0.00	0.000	-	0
4a	theta = 90°	0.00	0.000	-	0
4b	M1-M2 lower	0.00	0.000	-	0
5a	c = 0 bar	0.00	0.000	-	0
5b	φ_s = 20°	0.00	0.000	-	0
5c	φ_d = 10° ; d_c = 2 mm	0.00	0.000	-	0
5d	φ_d = 20° ; d_c = 20 mm	0.00	0.000	-	0
6a	E = 8 GPa	0.00	0.000	-	0
6b	E = 20 GPa	0.00	0.000	-	0
8	UGS ΔP1 = ΔP2 = -150 bar (mech 04)	0.00	0.000	-	0
9	salt caprock	0.00	0.000	-	0
1a	old reference	0.00	0.000	-	0
1d	new reference	0.00	0.000	-	0
5b WP3	c =100 bar	0.00	0.000	-	0

Table 7 Faults F2 and F3: ranking of the combination scenarios, from the most to the least prone to induce fault reactivation during cushion gas injection and UGS phases, using criterion 1(a). The same ranking is otained using criterion 1(b).

	Scenario #	χ_{max} UGS	Maximum δ_{avg}	Activation L.S.	χ_{max}
Fault F2	Comb1-WP3	0.86	0.012	9	1
	11	0.79	0.021	6	1
	10	0.78	0.006	7	1
	Comb2-WP3	0.77	0.021	8	1
	14	0.75	0.006	10	0.94
	12	0.74	0.026	8	1
	13	0.69	0.004	10	1
Fault F3	Comb2-WP3	1.00	0.020	5	1
	Comb1-WP3	0.95	0.041	6	1
	10	0.77	0.004	-	0.8
	11	0.72	0.010	10	1
	14	0.61	0.008	-	0.87
	12	0.59	0.013	-	0.78
	13	0.48	0.003	-	0.73

The modelling study reveals that fault reactivation may occur unexpectedly during cushion gas injection and UGS phase, following more expected reactivation during primary production. Generally, scenarios more prone to activation during PP are also the most critical ones during CG and UGS; indeed, the two proposed criteria, the first mainly focused on UGS response, the second on PP, provide a similar ranking. During UGS, fault activation may be induced more often at the end of the injection phase (i.e., at $P=P_{initial}$) and, secondarily, at the end of the production phase (at P_{min}). Notice that during UGS/CG the fault activates on a portion of the element patch that already slides during PP. However, sliding in CG/UGS usually occurs in the opposite direction compared to PP, following reservoir expansion.

5. Weighting the critical factors

Inspection of Table 3 – Table 6 reveals that the critical factors (drivers/settings) influencing fault activation during cushion gas injection and UGS cycles arrange differently for the boundary and central faults, F2 and F3.

On fault F2, i.e. for the faults bounding the reservoir, Table 3 and Table 4 reveal that during UGS the stability is mainly jeopardized by an initial stress regime with small horizontal principal components, failure criterion with low friction angle, large pressure change because of production/injection, and significant contrast between the reservoir and the over- side- and underburden stiffness.

Due to symmetry conditions of fault F3 for most of the scenarios, the major influencing drivers to fault instability are given by geometrical parameters characterizing the fault/reservoir system (Table

5 and Table 6). Offset of the reservoir compartments, non-vertical fault plane, different pressure change in the two compartments, and fault dip are the features threating the stability of the fault F3.

These considerations are supported by the ranking of the combined scenarios (Table 7): the most critical scenarios are characterized by a fault offset equal to reservoir thickness, small fault friction angle, an heterogeneous stiffness distribution, and a viscous caprock. Conversely, these factors lack in the less critical scenario 13.

6. Guidelines for safe operational bandwidths

After the end of primary production when the natural fluid pressure P_i is reduced to $P_{min,PP}$, UGS reservoirs experience a relatively fast pressure recovery to $P_{max,CG}$ during cushion gas injection and then a generally-seasonal pressure fluctuation during the UGS phase between $P_{min,UGS}$ and $P_{max,UGS}$ at the end of the production and injection phases, respectively. Usually, $P_{max,CG} \cong P_{max,UGS} \cong P_i$ and $P_{min,UGS} \geq P_{min,PP}$ (Figure 6).

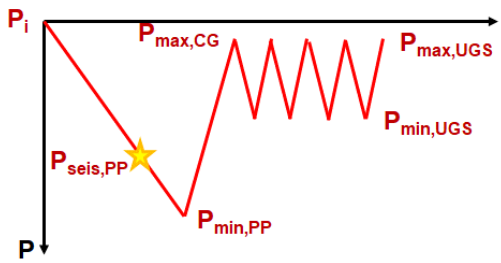

Figure 6 Pressure values used in the definition of the guidelines.

Guidelines for a "safe operation bandwidths" in UGS, i.e. UGS operations with a reduced risk of inducing seismicity, must provide proper bounds for the pressure values defined just above. Nevertheless, it must be recalled that a fault reactivation can occur aseismically.

The numerous scenarios investigated within the study have clearly revealed that fault reactivation is more likely to happen during cushion gas injection and UGS if i) reactivation has occurred during primary production and ii) when the reservoir pressure is approaching or reaches $P_{max,CG}$, $P_{max,UGS}$, and $P_{min,UGS}$. Fault reactivation is largely case-sensitive, depending on the geometry of the fault/reservoir (the presence of sloped faults, offset of the reservoir compartments), differential pore pressure between adjacent reservoir compartments and within each reservoir block, the geomechanical properties of the faults and the reservoir, caprock, under- and overburden.

Therefore, specific investigations are fundamental to characterize the reservoir setting and, to avoid or reduce the risk of critical operations. In particular, importance should be given to improve the knowledge on (from the most to the least importance):

- the initial stress regime on the faulting system;
- the reservoir compressibility;
- the geomechanical parameters of the faults (failure criterion);

- the reservoir permeability (or, equivalently, the pore pressure distribution within the reservoir compartment).

A few general guidelines can be derived as final outcome of this research. They are necessarily qualitative because of the theoretical/general framework of the modelling application, the quasi-static nature of the model implemented, which properly simulates fault slip but not seismicity, and the related consideration, already pointed out above, that fault failure can be aseismic (for example, according to Wassing et al. (2017), "*after the onset of fault reactivation, a further pore pressure decline of 3.7 MPa* (or 1.6 MPa with no fault offset) *and a critically stressed length of approximately 30 m is needed for the nucleation of a seismic event*"). The following "safe operation bandwidths" are suggested:

- If seismicity has been recorded during primary production, $P_{max,CG}$ and $P_{max,UGS}$ must be safely smaller than P_i. Indeed, a number of investigated scenarios (see for example Figure 30, WP6 Report) reveal that fault activation during primary production leads to a stress redistribution and a new deformed "equilibrated" configuration that is newly loaded, in the opposite direction (as the reservoir expands), when the pressure variation changes the sign. A reasonable rule is to keep the pressure recovery smaller than the minimum between $\theta\left|P_i - P_{seis,PP}\right|$ and $\left|P_i - P_{min,PP}\right|$, where $P_{seis,PP}$ is the pressure at the time of the (first) seismic occurrence (Figure 6) and θ a "form" factor, with $1 \leq \theta \leq 2$. With the assumptions used in this study (regular geologic setting, main stress orientation aligned with the fault systems, and uniform pressure change within the reservoir) $\theta = 2$, but it can be smaller in more realistic configurations. Generally, the first or the second bound prevails depending on the condition that $P_{seis,PP}$ is quite far from or close to $P_{min,PP}$;
- If seismicity has been recorded during primary prduction, $P_{min,UGS}$ must be safely bounded. During the UGS production phase, the stress acting on the faults varies "coherently" (as the reservoir compacts again) with the primary production phase, although starting from a different initial stress state. Therefore, if $P_{max,CG}$ meets the previous constraint, the pressure depletion during the UGS production phase must be kept smaller than $\left|P_{max,CG} - P_{min,PP}\right|$; if not (i.e., a fault reactivation has occurred also during cushion gas injection because the safety bound above has not been respected), then the pressure drop during UGS production must be kept smaller than $\theta\left|P_i - P_{seis,PP}\right|$, with the "form" factor θ in the range $1 \leq \theta \leq 2$ and, $\theta = 2$ with the assumptions used in this study. Notice that the bound must be given on the pressure drop and not to $P_{min,UGS}$ because this latter depends on the actual $P_{max,CG}$ value experienced by the reservoir;
- If seismicity has been recorded during primary production on an intra-reservoir fault, during cushion gas injection and UGS the pressure difference between the various reservoir compartments must be safely kept smaller than $\left|P_i - P_{seis,PP}\right|$. Scenario 7b (WP6 Report), for example, clearly highlights the validity of the statement;
- If no seismicity has been recorded during primary production, $P_{max,CG}$ can safely be equal to P_i. Indeed, the system behaves elastically, and the pressure recovery unloads the faults to their initial criticality condition;

- If no seismicity has been recorded during primary production and cushion gas injection, UGS pressure change can safely span the whole pressure change between P_i and $P_{min,PP}$. As above, the system behaves elastically within the pressure range experienced by primary production and cushion gas injection. Therefore, a UGS within the same range of pressure variation does not yield the system toward a more critical condition in terms of fault reactivation.

Finally, it must be emphasized that the above rules are aimed at avoiding (or at least limiting the possibility) of fault failure. Therefore, since reactivation can develop with aseismic slip, they can be considered conservative recommendations.